Equatorial spread F-related airglow depletions at Arecibo and conjugate observations

C. Martinis[1] and M. Mendillo[1]

[1]   We present evidence of the incursion into the Caribbean region of airglow depletions associated with the equatorial Rayleigh-Taylor instability. Data from the Boston University all-sky imager located at Arecibo, Puerto Rico (18.3°N, 66.7°W, 28°N magnetic latitude), have been used to identify several nights with 630.0 nm airglow patterns that are typical signatures of equatorial spread F and distinctly different from the more common "airglow bands" frequently observed there. Two case studies (2 November 2002 and 26 February 2003) show the occurrence of simultaneous airglow depletions observed with another all-sky imager located at El Leoncito, Argentina (31.8°S, 69.3°W, 18°S magnetic latitude), relatively close to the Arecibo conjugate point. Supporting information is obtained from Defense Meteorological Satellite Program, ROCSAT-1, and GPS data, all of them showing the presence of strong ionospheric irregularities collocated with the airglow depletions. Mapping the circular field of view from Arecibo into the Southern Hemisphere reveals a distorted pattern due to the differences in the magnetic field characteristics in both hemispheres. This adds an interesting spatial complexity to the formulation of conjugate point observing programs in the Latin American longitude sector.

Citation: Martinis, C., and M. Mendillo (2007), Equatorial spread F-related airglow depletions at Arecibo and conjugate observations, *J. Geophys. Res.*, *112*, A10310, doi:10.1029/2007JA012403.

1. Introduction

[2]   An all-sky camera was installed by the Boston University Imaging Group at Arecibo, Puerto Rico (18.3°N, 66.7°W, 28°N magnetic latitude), for campaign mode observations in 1990 and 1995 and then permanently in 2002 (quick look images can be found at www.buimaging.com). The Caribbean region hosts a variety of thermospheric/ionospheric processes mostly dominated by the electrodynamics of a midlatitude region (20–30° magnetic latitude) with a large magnetic inclination angle ($I \sim 50°$). Thus Arecibo, in general, is not affected by the electrodynamical processes typically occurring in the equatorial/low-latitude ionosphere. However, it is well known that the Arecibo region spans the strong latitude gradient toward the northern crest of the equatorial ionization anomaly (EIA) [*Wright*, 1960; *Aponte et al.*, 2000]. One example of the intrusion into the midlatitude domain of typical equatorial/low-latitude processes is found in the well-known midnight collapse observed at Arecibo [*Nelson and Cogger*, 1971; *Mendillo et al.*, 1997]. This phenomenon, related to the presence of a temperature maximum at the equator, is responsible for changes in the direction and intensity of meridional winds [*Meriwether et al.*, 1986]. *Martinis et al.* [2006] showed the simultaneous occurrence of the optical signature of the midnight collapse as a brightness wave in 630.0 nm airglow emissions at Arecibo and El Leoncito, Argentina (31.8°S, 69.3°W, 18°S magnetic latitude). These observations, along with the occurrence of airglow depletions associated with equatorial spread F (ESF), are examples of the intrusion of low-latitude processes (L values <1.2) into the midlatitudes domain ($L \sim 1.4$). This coupling does not occur very frequently and the thermospheric and ionospheric conditions leading to it are not fully understood.

[3]   The most typical 630.0 nm signatures at Arecibo are "airglow bands" moving southwestward [*Mendillo et al.*, 1997; *Miller et al.*, 1997; *Garcia et al.*, 2000]. These are associated with changes in electron density heights and, in general, make a large angle with respect to the magnetic meridian. Although not completely understood, evidence exists supporting the role of the Perkins instability and polarization electric fields as the responsible mechanism of the features observed [*Perkins*, 1973; *Benkhe*, 1979; *Kelley et al.*, 2002a]. Another type of observations is the occurrence of "poleward surges" as defined by *Kelley et al.* [2000]. These surges are observed as depletions in airglow images piercing Arecibo's field of view (FOV) from the south. They are more structured than the airglow bands and are accompanied by large total electron content (TEC) variations, affecting the radio waves traversing the ionosphere. Their observation has coincided with high magnetic activity periods. They tend to show closer alignment with the magnetic meridian than the airglow bands.

[1]Center for Space Physics, Boston University, Boston, Massachusetts, USA.

[4] A visually distinct feature, airglow depletions associated with ESF, typically occurs at much lower latitudes. Yet, using observations from Arecibo, *Mendillo et al.* [1997] proposed that the ESF's optical signatures can reach into lower midlatitudes. There has been some reluctance to accept that ESF could reach Arecibo latitudes. Many of the signatures of poleward surges are similar to the ones produced by ESF-related airglow structures. For example, the case reported as an ESF-related depletion by *Mendillo et al.* [1997] was later interpreted as a midlatitude poleward surge by *Kelley et al.* [2000]. In this paper we will show results indicating the occurrence of airglow depletions associated with low-latitude instabilities (ESF) at Arecibo.

2. Coupled Latitude-Altitude Nature of ESF

[5] Ionospheric irregularities associated with the equatorial Rayleigh-Taylor instability (RTI), commonly known as ESF, occur after sunset and can reach very high altitudes at the magnetic equator. Because of the flux tube nature of the RTI process, high-altitude ESF structures map to latitudes away from the equator. When using all-sky imaging systems, they can be sampled as depletions in the 630.0 nm airglow emission. *Mendillo et al.* [2005] used buoyancy arguments to suggest that a depleted flux tube in the bottomside *F* layer due to ESF would rise to an apex height where it is equal to the background flux tube integrated electron density. In addition to the case studies from radars, imagers, and satellite data discussed by *Mendillo et al.* [2005], depletions reaching heights $\geq$1500 km have been observed in Brazil [*Sahai et al.*, 1994, 2000], Hawaii [*Kelley et al.*, 2002b], Argentina [*Martinis et al.*, 2006], and at conjugate locations in Japan and Australia [*Otsuka et al.*, 2004]. *Sahai et al.* [2000] also showed that plasma bubbles reaching very high apex heights (>500 km) at the magnetic equator were more abundant during high solar activity (66%) compared with low solar activity (34%).

[6] Depletions observed near the magnetic equator show a very close alignment with the magnetic meridian and do not exhibit the high level of structuring present in higher-latitude depletions. At higher latitudes they have been observed to tilt toward the west [*Mendillo and Tyler*, 1983; *Makela and Kelley*, 2003]. This is a consequence of latitudinal gradients in the zonal neutral winds that tend to be slower near the crests of the EIA. They generate nighttime *F* region drifts, and structures embedded therein move slower when compared to behavior near the magnetic equator [*Martinis et al.*, 2003; *Pimenta et al.*, 2003]. This produces a departure from the close alignment with the magnetic meridian. Yet the ESF-related airglow depletions and the poleward surges are more aligned with the magnetic meridian when compared to the airglow bands. They both present strong TEC fluctuations when observed by GPS satellites. The poleward surges have been reported to move westward, while ESF-related depletions typically move eastward. However, when magnetic activity is high, the ESF-related depletions can also move westward. High magnetic activity appears to be a necessary condition to observe the westward moving poleward surges [*Kelley et al.*, 2000]. While we tend to equate poleward surges and the "intrusion of ESF toward Arecibo," further studies, includ-ing conjugate observations, are needed to understand if these processes are related or are different by nature.

3. Instrumentation and Data

[7] The Arecibo system was installed in May 2002 and utilizes a bare charged coupled device (CCD) detector behind a rotating filter wheel which houses up to six narrowband (1.2–1.8 nm full width at half maximum) filters. The filters record oxygen emissions from several height regimes: mesospheric $O(^1S)$ from 557.7 nm near 96 km in altitude and thermospheric $O(^1D)$ 630.0 nm emission from ~250 to 300 km. A filter centered at 644.4 nm is used to monitor continuum emission. Most of the thermospheric features observed at this station can also be attributed to typical midlatitude thermosphere-ionosphere processes. Yet winds caused by the midnight temperature maximum at equatorial regions routinely reach Arecibo causing the "brightness waves" observed by all-sky imagers [*Mendillo et al.*, 1997; *Colerico and Mendillo*, 2002]. We will focus on the effects of the RTI in the Caribbean. Although this instability is originated at equatorial/low latitudes, its effects can reach the Arecibo region.

[8] In South America, Boston University operates another imager at El Leoncito, Argentina (31.8°S, 69.3°W, 18°S magnetic latitude), located close to the crest of the EIA. It can be considered a low-latitude site, with frequent occurrence of airglow depletions associated with the RTI. A study by *Martinis et al.* [2006] showed that airglow depletions can extend to the southern edge of the imager FOV, meaning that the apex height can reach heights >1800 km. The all-sky imager at El Leoncito was installed in early 2000 after being moved from its previous location at Tucuman [*Martinis et al.*, 2003]. It consists of an intensified CCD system with a five position filter wheel that provides information at 630.0, 557.7, and 777.4 nm. These emissions are used for mesospheric [*Smith et al.*, 2003] as well as thermospheric studies [*Martinis et al.*, 2006]. We will use observations from this station and from Arecibo to show the simultaneous occurrence of airglow depletions associated with the RTI.

[9] For specific case studies we will use data from the Defense Meteorological Satellite Program (DMSP) satellites that provide in situ ion density measurements at ~840 km in a high-inclination orbit. Ion density data from ROCSAT-1, a satellite orbiting in a 35° inclination angle at ~580 km, will also be used. ROCSAT-1 provides information on the east–west extent of the irregularities in the evening hours, while DMSP satellites sample the ionosphere in an almost north–south trajectory. GPS data from the International GNSS Service (IGS) network are processed to obtain phase fluctuations that can be used as a measure of ionospheric irregularities [*Mendillo et al.*, 2000].

[10] Figure 1 shows a map indicating the location of the instruments at Arecibo, Puerto Rico, and El Leoncito, Argentina. Magnetic latitudes and magnetic longitudes are indicated as solid and dotted lines, respectively. The circles show the 150° FOV of the instruments at a height of 300 km. The dashed oval indicates the mapped FOV of the circle centered at Arecibo. This was obtained by mapping the geographic coordinates of the 150° FOV circle into the Southern Hemisphere using the International Geomagnetic Reference Field 10 model and magnetic apex coordinates
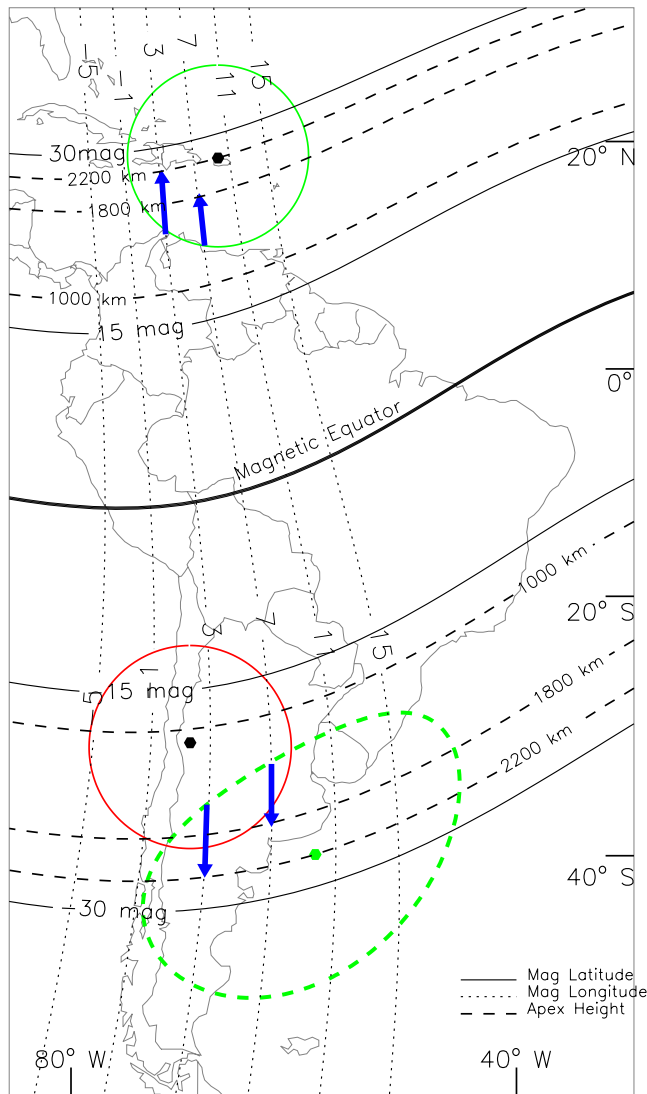
Figure 1. Map of South America and the Caribbean showing the location of the Arecibo and El Leoncito imagers. Circles represent 150° FOVs. Dashed oval indicates the mapped FOV of Arecibo. Dashed lines represent apex heights. Solid lines indicate magnetic latitude. Dotted lines show magnetic longitudes. Blue arrows show how structures map from one hemisphere to another. Notice the differences between geographic latitudes and geomagnetic latitudes at both sites.

[*Richmond*, 1995]. The unique geometry of the magnetic field in this region produces this effect, very different from the more regular pattern existing, for example, in the Australasian sector, where the mapping of a circular FOV also produces a circle [*Otsuka et al.*, 2004]. Figure 1 also shows apex height curves (dashed lines). A field line at 300 km at El Leoncito's zenith reaches a height of ∼1000 km at the magnetic equator. If depletions are observed reaching the southern edge of the field of view, then irregularities at the equator have reached heights >1800 km. For Arecibo at 300 km at zenith a magnetic field line reaches 2200 km at the magnetic equator. The blue arrows drawn at 3 and 7° magnetic longitudes show how

structures map from one hemisphere to another for flux tubes that are common to both sites. We see from Figure 1 that the southwest portion of Arecibo's FOV corresponds to the southeast region of the El Leoncito FOV.

[11] Figure 2 shows the simultaneous detection of ESF-related airglow depletions using the all-sky imagers located at Arecibo (top) and at El Leoncito (bottom) on the night of 26 February 2003. Quiet geomagnetic conditions are observed in this night with $\langle Kp \rangle \sim 2$, $Dst \sim 2$ nT, and interplanetary magnetic field (IMF) Bz ~ 2 nT. North is at the top of the images, and east is to the right. Arecibo images show three small depletions piercing from the south and moving eastward. At El Leoncito, very large depletions were observed the entire night, but those leaving the southern part of the FOV (and thus belonging to flux tubes with apex heights high enough to be observed at Arecibo) were seen only until ∼0400 UT. The overall behavior in both ionospheres, with multiple narrow depletions at El Leoncito moving eastward and then appearing at Arecibo, indicates that we are seeing common features. Because of the longitudinal offset of the two imagers and distortion effects near the horizon we can compare only a few individual structures seen at both sites. For example, by 0258 UT Arecibo shows two depletions, but only the one located most to the west is observed simultaneously at El Leoncito, close to the eastern horizon.

[12] Figure 3 shows another case of simultaneous occurrence of ESF-type airglow depletions on the night of 2 November 2002. For this night, $\langle Kp \rangle$ was ∼ 4, $Dst \sim -25$ nT, and IMF Bz slightly southward (∼−4 nT). The eastward motion of the Arecibo depletions is evident. El Leoncito's imager also detected eastward motion of a large depletion (Figure 3 bottom (0038 UT)) that approaches the eastern edge of the FOV at 0058 UT. This depletion corresponds to the small dark feature observed at the western part of the Arecibo FOV at the same time (0059 UT). Although no new features are observed at Arecibo entering from the west after 0200 UT, El Leoncito showed weak depletions reaching to the zenith and thus were not able to reach apex heights corresponding to the southern edge of the Arecibo FOV.

[13] Figure 4 top shows results from GPS receivers in Puerto Rico (with station name PUR3) for the night of 2 November 2002, and Figure 4 bottom shows results from GPS receivers in Saint Croix (CRO1) for 26 February 2003. Figure 4 left indicates the 150° FOV of the GPS receivers at a height of 350 km and the subionospheric points versus UT for the satellites observed. For the February case (Figure 4 bottom), decreases in the equivalent vertical TEC (Figure 4 middle) and strong phase fluctuations or rate of change of TEC (Figure 4 right) are observed starting a 0400 UT, indicating the presence of irregularities. The all-sky imager data for this night showed depletions moving eastward and reaching the bottom half of the FOV, coinciding with the GPS observations. Figure 4 top shows similar plots for the night of 2 November 2002 for the GPS receiver at PUR3 and satellite 13. The region sampled is collocated with a depletion leaving the eastern part of the Arecibo FOV (see Figure 3).

[14] Figure 5 shows additional examples of 630.0 nm all-sky images observed at Arecibo with typical signatures of ESF-related airglow depletions: relatively closer alignment with the magnetic meridian and highly structured shape
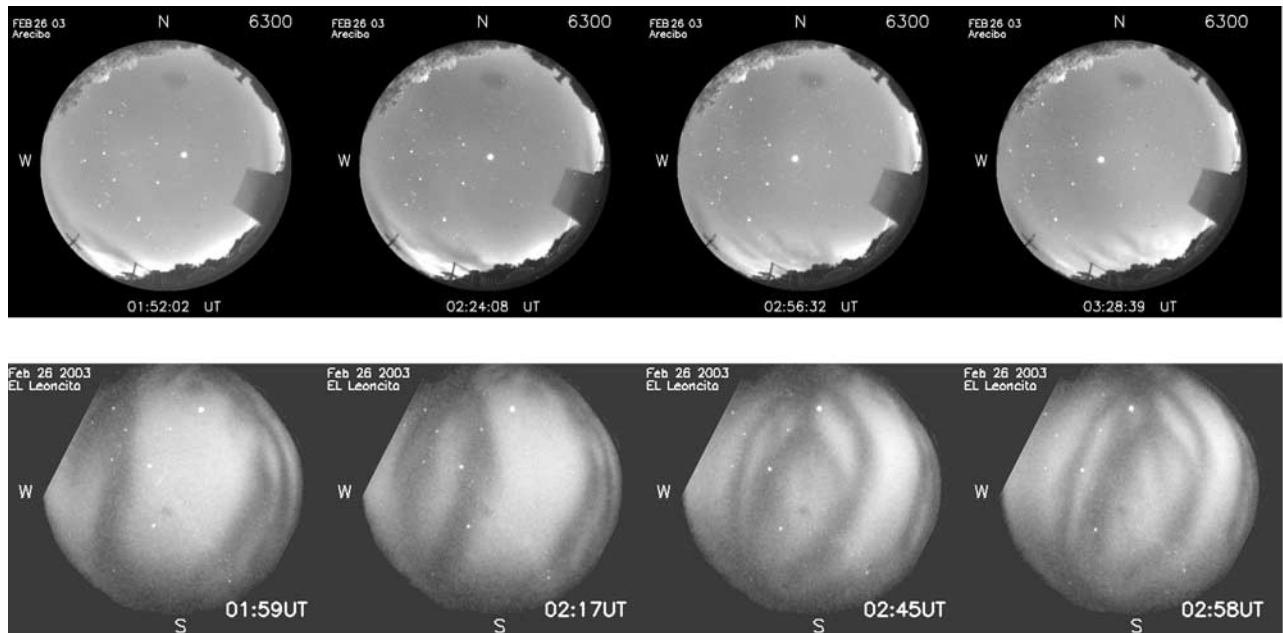
Figure 2. (top) Arecibo images for the night of 26 February 2003; three small depletions moving eastward are seen piercing into the southern FOV. (bottom) Same night at El Leoncito; depletions were observed all night, but those reaching the southern FOV occurred only from ~0130 to 0400 UT. Only the structures east from the center of the images at 0217 and 0258 UT are the ones appearing at Arecibo. Large wishbone-like structure seen at El Leoncito at 0258 UT does not reach the southern FOV and thus it is not observed at Arecibo.

(that distinguish them from the typical airglow bands), and post-sunset occurrence. The cases shown in Figure 5 top correspond to relatively quiet magnetic activity ($\langle Kp \rangle$ = 3) where the motion of the depletions is eastward (not shown).

The cases shown in Figure 5 bottom occurred during high magnetic activity ($\langle Kp \rangle$ = 6) and their motion is westward (not south-westward, as the typical airglow bands motion), a consequence of disturbance dynamo effects that reverse the
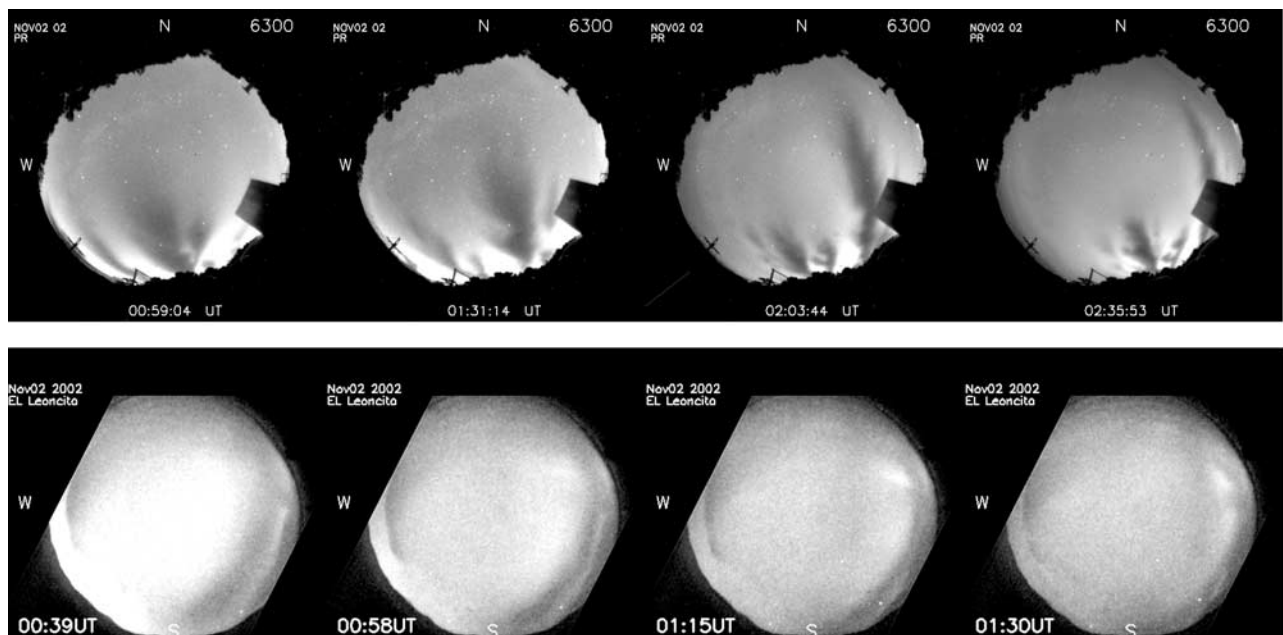

Figure 3. (top) Arecibo images for 2 November 2002. Airglow depletions are moving eastward. (bottom) Same night at El Leoncito. Large airglow depletion is seen moving eastward, leaving the eastern part of the FOV. Structure seen toward the southwest at Arecibo at 0059 UT (first image at the top) is the same depletion observed at El Leoncito at 0058 UT (second image at the bottom).
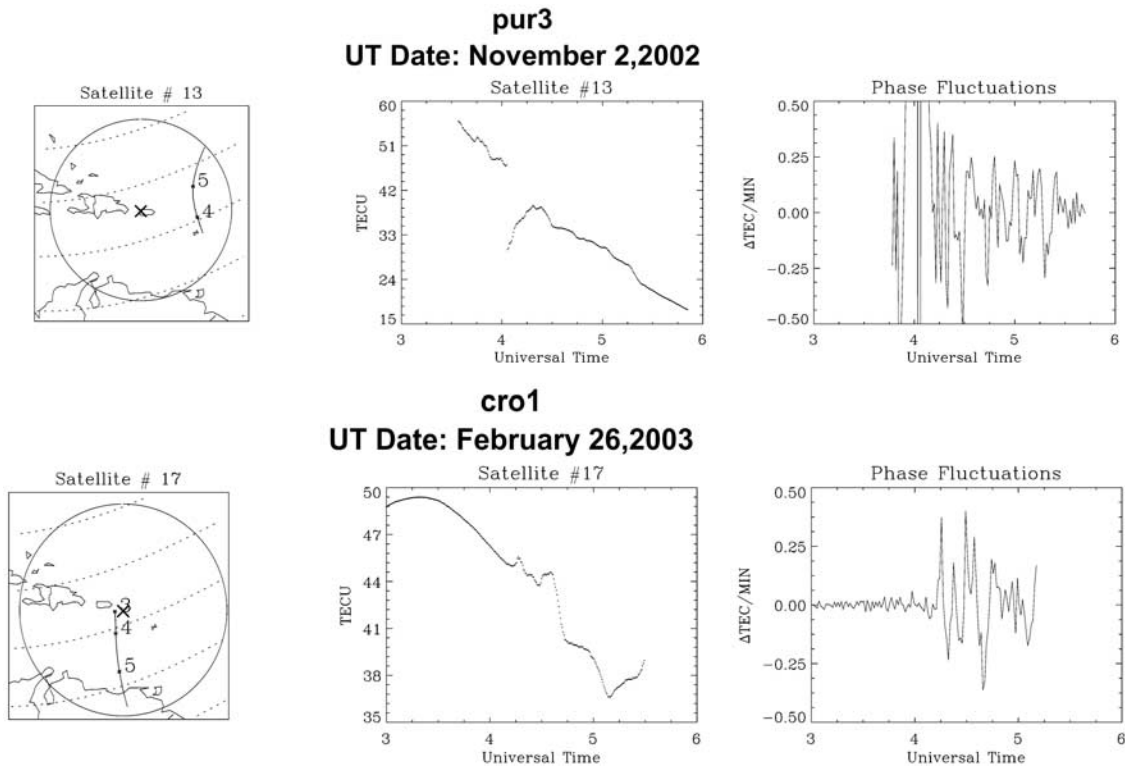
Figure 4. Data from GPS stations (top) PUR3 for 2 November 2002 and (bottom) CRO1 for 26 February 2006. (left) Maps with the station locations and FOVs. Numbered lines indicate the subionospheric points of the satellites trajectories with the numbers showing UT. (middle) Plots of equivalent vertical TEC values (the missing data at the bottom indicate loss of lock of the satellite signal). (right) Phase fluctuations (rate of change of TEC) data, with large values after ~0330 (top right) and 0400 UT (bottom right).
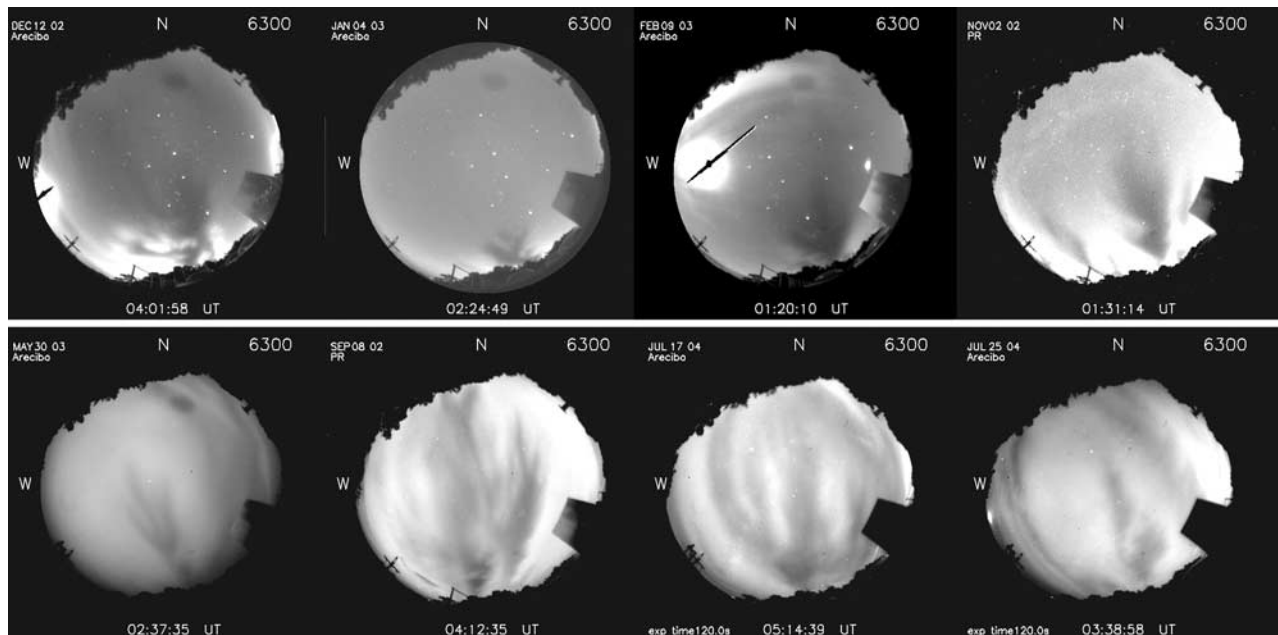

Figure 5. Examples at different nights of ESF-related depletions. (top) Eastward moving depletions during quiet time conditions ($\langle Kp \rangle \approx 3$). (bottom) Different nights with depletions reaching the northern FOV of the imager during geomagnetic disturbed conditions ($\langle Kp \rangle \approx 6$); these cases showed westward motion.
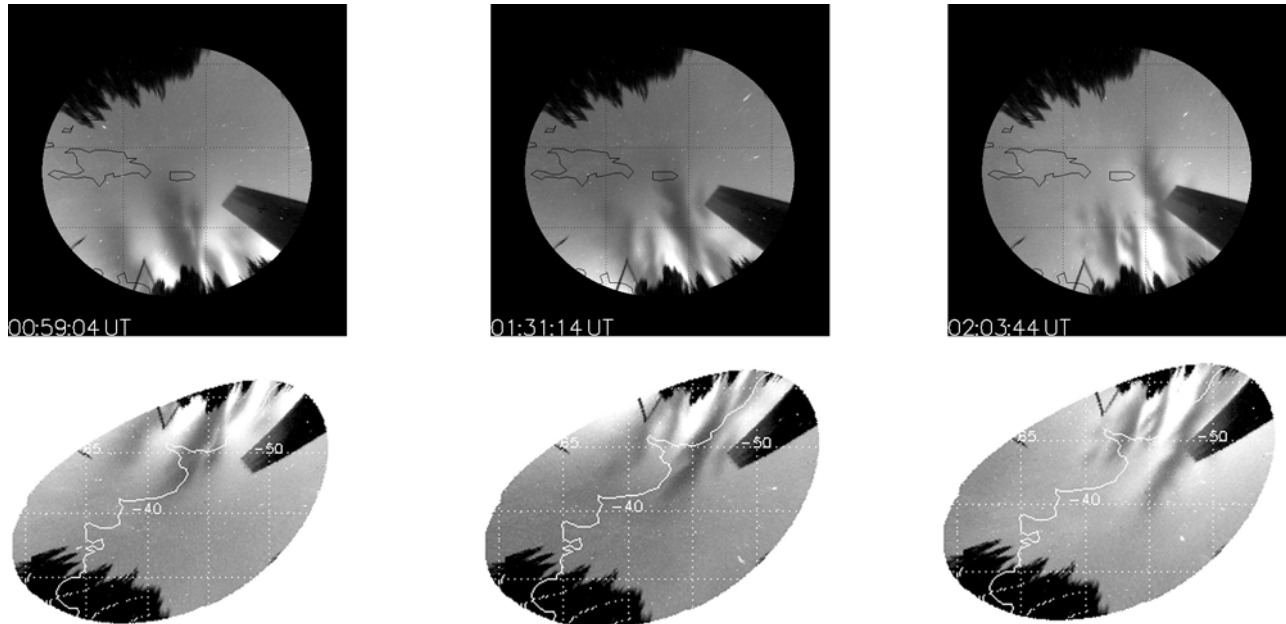
Figure 6. (top) Unwarped Arecibo images for 2 November 2002, assuming a 300 km emission height, showing eastward motion. (bottom) Respective conjugate images resulting from mapping the unwarped Arecibo images into the Southern Hemisphere.

direction of plasma motion [*Taylor et al.*, 1997; *Fejer*, 2002].

[15] The cases presented here are indicative of Arecibo airglow depletions associated with the equatorial RTI. In general, most of the depletions are observed in the bottom half of the imager's FOV, meaning that the apex heights are limited to values less than ~2200 km.

4. Magnetic Field Mapping and Further Evidence of Conjugate Phenomena

[16] The two case studies presented in Figures 2 and 3 show the occurrence of airglow depletions at Arecibo and El Leoncito. In order to portray how well these observations are related geomagnetically we mapped the Arecibo images observed on 2 November 2002 into the Southern Hemisphere. First, we convert the raw images into a latitude-longitude array using a FOV of 150° (to avoid distortion effects near the horizon) assuming a uniform emission height of 300 km. The pixel positions in the new "unwarped" images now have latitude and longitude information. Next, given the geographic location of every pixel in the unwarped image, we calculate their respective magnetic conjugate latitude and longitude and assign a pixel position to this new image. As a result, a conjugate mapped all-sky image is obtained. Figure 6 shows Arecibo images that were unwarped (top) and the corresponding images obtained when they are mapped into the Southern Hemisphere (bottom). Notice how distorted the individual depletion orientations are when mapped into the Southern Hemisphere. This is a direct consequence of the peculiar behavior of the Earth's magnetic field at this longitude sector. Similarly, a circular FOV in the Southern Hemisphere would map into the Northern Hemisphere into an oval elongated in the north–south direction.

[17] Figure 7 shows a map of South America and the Caribbean with the Arecibo image at 0059 UT on 2 November 2002 mapped to its conjugate location in the Southern Hemisphere. The map clearly shows the overlapping region that exists between the El Leoncito imager (indicated in Figure 7 with the 150° circular FOV) and the conjugate image from Arecibo. The small depletion observed to the south–west in the Arecibo image (north–west in the mapped image) is inside the circle representing the El Leoncito imager, matching the structure observed there in Figure 3. This portrayal of geometry shows that even though the magnetic declination at ~65°W and ~35°S (the approximate location of the common area) is very small (~1°) the structures show a tilt toward the west, a clear indication of latitudinal gradients in zonal plasma drifts [*Mendillo and Baumgardner*, 1982; *Anderson et al.*, 1987].

[18] In situ ion density data from DMSP F14 and ROCSAT-1 satellites are also available for this night. The trajectories during this night are shown in Figure 7, and the data are presented in Figure 8. DMSP F14 moved northward in an orbit that was in the longitudinal sector corresponding to the common area observed by the imagers. Before crossing the magnetic equator, bubbles are detected in the latitudinal range of −20 to −10° magnetic latitude, meaning that these irregularities occur as high as 1800 km at the magnetic equator. When it crosses the magnetic equator, at 0053 UT, more plasma bubbles were observed. These bubbles map along the magnetic field lines to a geographic latitude of ~−28° in the Southern Hemisphere at ~300 km, with the footprint of the field lines corresponding to the region covered by the El Leoncito imager that detected airglow depletions (Figure 3). When the satellite reached the Northern Hemisphere, a large plasma bubble was observed between 5 and 10° magnetic latitude; this bubble is related to the structure observed at El Leoncito. By the time it
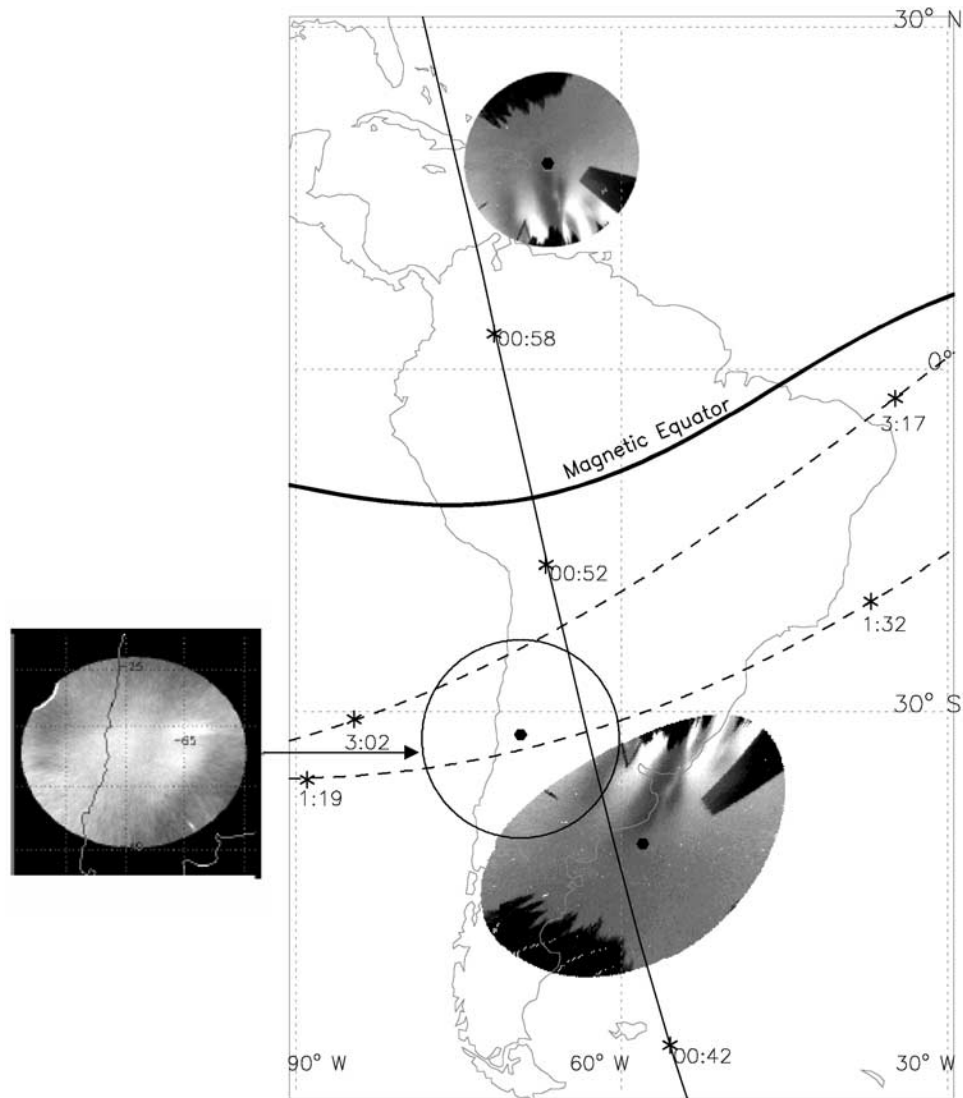
Figure 7. (right) Map of Latin America showing an unwarped Arecibo image (top) for 2 November 2002 at 0059 UT, as well as the conjugate image mapped into the Southern Hemisphere (bottom). (left) A simultaneous image from El Leoncito shows a region of 630.0 nm depletion coincident with the mapped Arecibo image. Also shown here are the northward trajectory of DMSP F14 (solid line) and the eastward trajectory of two ROCSAT-1 passes (dashed lines). Stars indicate the UT locations of the satellites.

reaches the Caribbean region, no more in situ irregularities are measured because they are located to the east in the FOV of the Arecibo imager, while DMSP F14 passed to the west of Arecibo's FOV.

[19] ROCSAT-1 was moving eastward as it crossed the South American sector between ∼0120 and 0130 UT at ∼−30° latitude and detected two large plasma bubbles. The first drop in density (at ∼295−300° longitude) corresponds to the one that was captured by both imagers (see Figure 3). The second one (∼305° longitude) was observed only by the Arecibo imager, as can be inferred from the mapped image (shown in Figure 6 middle). Thus the two bubbles measured by ROCSAT-1 correspond to the two depletions observed in the mapped FOV of Arecibo in Figure 6 at 0130 UT. The next ROCSAT-1 pass in the South American sector shows very active conditions eastward from 295° longitude between ∼0310 and 0325 UT. A plasma bubble is

observed at 290° longitude. An airglow depletion associated with this bubble was detected by the El Leoncito imager, but it only extended to the zenith, and thus it could not be detected by the Arecibo imager. We conclude that this is a very active night for ESF with airglow depletions, TEC fluctuations, and density dropouts observed in the ∼290−340° longitudinal range in both hemispheres, all ordered in space by geomagnetic field topology.

5. Summary

[20] We have shown that airglow structures associated with ESF can occur in the Caribbean region, meaning that the apex heights of the irregularities can reach ∼2200 km. Two case studies from Arecibo and El Leoncito provided the necessary arguments of simultaneity to interpret the structures observed as being a flux-tube-dominated process.
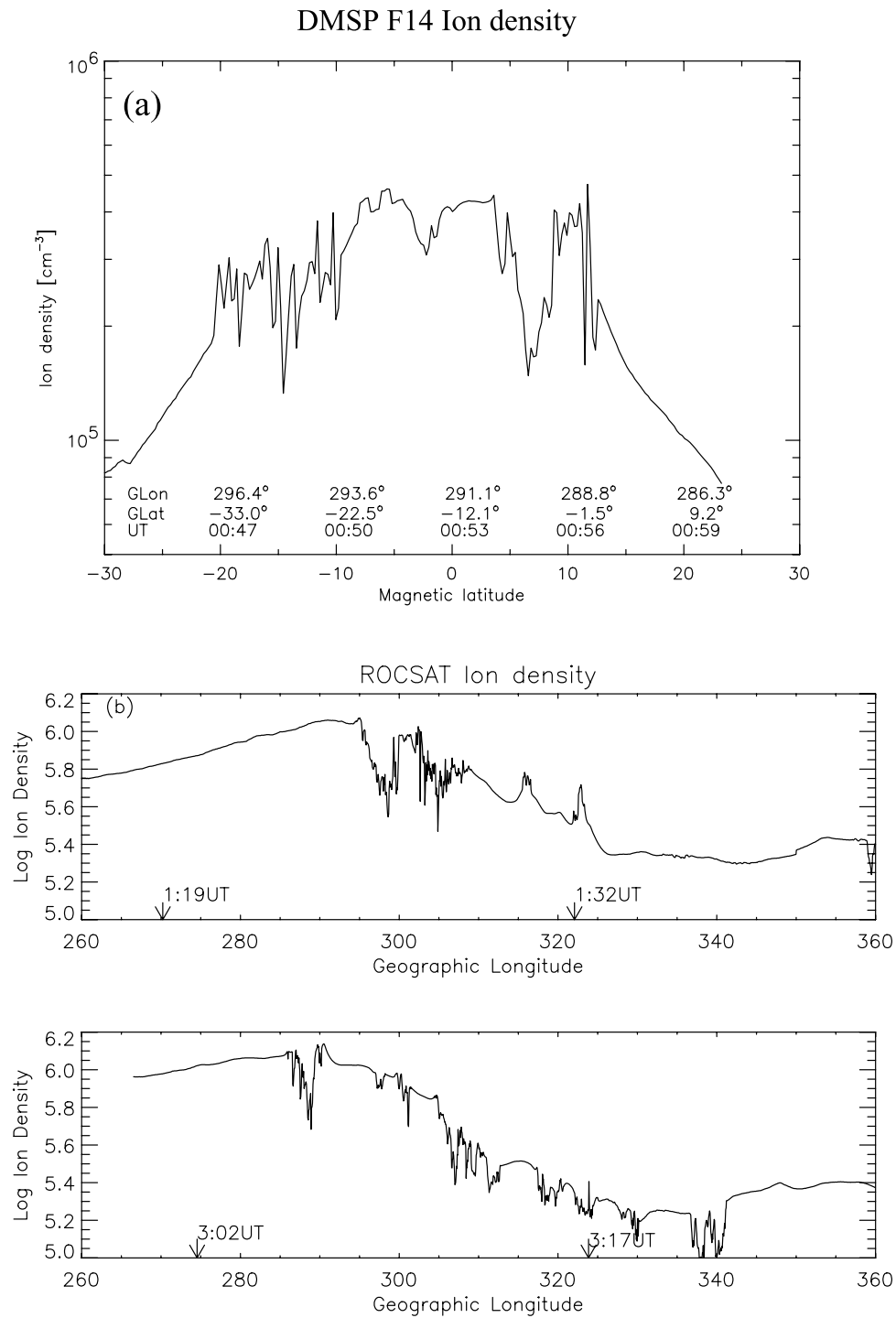
DMSP F14 Ion density

ROCSAT Ion density

Figure 8. (a) DMSP F14 ion density for a pass on 2 November 2002 in the South American sector. The region between −20 and 12° magnetic latitude shows the presence of plasma irregularities. (b) ROCSAT-1 data for two passes in the same region: (top) First pass shows two large plasma bubbles between 290 and 310° longitude that correspond to the depletions observed in the mapped Arecibo images (see Figure 6); (bottom) next pass in the sector shows perturbed conditions eastward of 290° longitude. Arrows in both passes indicate the UT and geographic latitude of the trajectories shown in Figure 7.

Supporting information from GPS data in Puerto Rico and Saint Croix showed the occurrence of strong phase fluctuations in the region where depletions were observed. In situ density data provided additional confirmation of the nature of the structures observed by the all-sky imagers, clearly indicating the presence of strong plasma bubbles. The mapping from one hemisphere to another was shown to be a complex process, and this is something that will need to be taken into

account very carefully in the formulation of conjugate observing programs in the American longitude sector.

[21] Arecibo's location can play a pivotal role in attempts to understand how low- to midlatitude coupling occurs. The region poleward of $\sim18°$ magnetic latitude and equatorward of $\sim25°$ magnetic latitude can be considered a good example of a transition region in which low-latitude processes can be seen extending to midlatitudes. From the theoretical point of view it is not clear what the required processes and/or parameters are to have an equatorial plasma bubble rise to more than 2000 km at the magnetic equator. Some cases observed at Arecibo occurred when magnetic activity was moderate to high, but we show here examples during relatively quiet conditions. It is also not clear how the inherently flux tube nature of the process is affected when very high apex heights are reached. How important are the conditions in the local ionosphere at latitudes poleward from the crests of the anomaly? Basic ESF theory always starts with a seed perturbation near the geomagnetic equator, and then because of the high conductivity along field lines the perturbation evolves as a bihemispheric structure, i.e., as a flux tube interchange instability. The question remains open concerning local (single-hemisphere) influences that, again, because of field line mapping, can appear in the conjugate regions. Such effects are not in classic ESF/RTI processes treated to date.

References

Anderson, D. N., R. A. Heelis, and J. P. McClure (1987), Calculated night-time eastward plasma drift velocities at low latitudes and their solar cycle dependence, *Ann. Geophys.*, 5, 435–442.

Aponte, N., S. A. González, M. C. Kelley, C. A. Tepley, X. Pi, and B. Iijima (2000), Advection of the equatorial anomaly over Arecibo by small-storm related disturbance dynamo electric fields, *Geophys. Res. Lett.*, 27, 2833–2836.

Benkhe, R. (1979), F layer height bands in the nocturnal ionosphere over Arecibo, *J. Geophys. Res.*, 84, 974–978.

Colerico, M., and M. Mendillo (2002), The current state of investigations regarding the thermospheric midnight temperature maximum (MTM), *J. Atmos. Sol. Terr. Phys.*, 64, 1361–1369.

Fejer, B. (2002), Low latitude storm time ionospheric electrodynamics, *J. Atmos. Sol. Terr. Phys.*, 64, 1401–1408.

Garcia, F. J., M. C. Kelley, J. J. Makela, and C.-S. Huang (2000), Airglow observations of mesoscale low-velocity traveling ionospheric disturbances at midlatitudes, *J. Geophys. Res.*, 105, 18,407–18,416.

Kelley, M. C., F. Garcia, J. Makela, T. Fan, E. Mak, C. Sia, and D. Alcocer (2000), Highly structured tropical airglow and TEC signatures during strong geomagnetic activity, *Geophys. Res. Lett.*, 27, 465–468.

Kelley, M., J. Makela, and A. Saito (2002a), The mid-latitude F region at the mesoscale: Some progress at last, *J. Atmos. Sol. Terr. Phys.*, 64, 1525–1529.

Kelley, M. C., J. J. Makela, B. M. Ledvina, and P. M. Kintner (2002b), Observations of equatorial spread F from Haleakala, Hawaii, *Geophys. Res. Lett.*, 29(20), 2003, doi:10.1029/2002GL015509.

Makela, J. J., and M. C. Kelley (2003), Field-aligned 777.4-nm composite airglow images of equatorial plasma depletions, *Geophys. Res. Lett.*, 30(8), 1442, doi:10.1029/2003GL017106.

Martinis, C., J. V. Eccles, J. Baumgardner, J. Manzano, and M. Mendillo (2003), Latitude dependence of zonal plasma drifts obtained from dual-site airglow observations, *J. Geophys. Res.*, 108(A3), 1129, doi:10.1029/2002JA009462.

Martinis, C., J. Baumgardner, S. M. Smith, M. Colerico, and M. Mendillo (2006), Imaging science at El Leoncito, Argentina, *Ann. Geophys.*, 24, 1375–1385.

Mendillo, M., and J. Baumgardner (1982), Airglow characteristics of equatorial plasma depletions, *J. Geophys. Res.*, 87, 7641–7652.

Mendillo, M., and A. Tyler (1983), Geometry of depleted plasma regions in the equatorial ionosphere, *J. Geophys. Res.*, 88, 5778–5782.

Mendillo, M., J. Baumgardner, D. Nottingham, J. Aarons, B. Reinisch, J. Scali, and M. Kelley (1997), Investigations of thermospheric-ionospheric dynamics with 6300-A images from the Arecibo Observatory, *J. Geophys. Res.*, 102, 7331–7344.

Mendillo, M., B. Lin, and J. Aarons (2000), The application of GPS observations to equatorial aeronomy, *Radio Sci.*, 35, 885–904.

Mendillo, M., E. Zesta, S. Shodhan, P. J. Sultan, R. Doe, Y. Sahai, and J. Baumgardner (2005), Observations and modeling of the coupled latitude-altitude patterns of equatorial plasma depletions, *J. Geophys. Res.*, 110, A09303, doi:10.1029/2005JA011157.

Meriwether, J. W., J. W. Moody, M. A. Biondi, and R. J. Roble (1986), Optical interferometric measurements of nighttime equatorial thermospheric winds at Arequipa, Peru, *J. Geophys. Res.*, 91, 5557–5566.

Miller, C. A., W. E. Swartz, M. C. Kelley, M. Mendillo, D. Nottingham, J. Scali, and B. Reinisch (1997), Electrodynamics of midlatitude spread F 1. Observations of unstable, gravity wave-induced ionospheric electric fields at tropical latitudes, *J. Geophys. Res.*, 102, 11,521–11,532.

Nelson, G. J., and L. L. Cogger (1971), Dynamical behavior of the night-time ionosphere over Arecibo, *J. Atmos. Sol. Terr. Phys.*, 33, 1711–1726.

Otsuka, Y., K. Shiokawa, T. Ogawa, and P. Wilkinson (2004), Geomagnetic conjugate observations of medium-scale traveling ionospheric disturbances at midlatitude using all-sky airglow imagers, *Geophys. Res. Lett.*, 31, L15803, doi:10.1029/2004GL020262.

Perkins, F. (1973), Spread F and ionospheric currents, *J. Geophys. Res.*, 78, 218–226.

Pimenta, A. A., J. A. Bittencourt, P. R. Fagundes, Y. Sahai, R. A. Buriti, H. Takahashi, and M. J. Taylor (2003), Ionospheric plasma bubble zonal drifts over the tropical region: A study using OI 630 nm emission all-sky images, *J. Atmos. Sol. Terr. Phys.*, 65, 1117–1126.

Richmond, A. D. (1995), Ionospheric electrodynamics using magnetic apex coordinates, *J. Geomagn. Geoelectr.*, 47, 191–212.

Sahai, Y., J. Aarons, M. Mendillo, J. Baumgardner, J. A. Bittencourt, and H. Takahaski (1994), OI 630 nm imaging observations of equatorial plasma depletions at 16°S dip latitude, *J. Atmos. Sol. Terr. Phys.*, 56, 1461–1475.

Sahai, Y., P. R. Fagundes, and J. A. Bittencourt (2000), Transequatorial F region ionospheric plasma bubbles: Solar cycle effects, *J. Atmos. Sol. Terr. Phys.*, 62, 1377–1383.

Smith, S. M., M. J. Taylor, G. R. Swenson, C. She, W. Hocking, J. Baumgardner, and M. Mendillo (2003), A multidiagnostic investigation of the mesospheric bore phenomenon, *J. Geophys. Res.*, 108(A2), 1083, doi:10.1029/2002JA009500.

Taylor, M. J., J. V. Eccles, J. LaBelle, and J. H. A. Sobral (1997), High resolution OI (630 nm) image measurements of F region depletion drifts during the Guará campaign, *Geophys. Res. Lett.*, 24, 1699–1702.

Wright, J. W. (1960), A model of the F region above $h_{max}F_2$, *J. Geophys. Res.*, 65, 185.

————————
C. Martinis and M. Mendillo, Center for Space Physics, Boston University, 725 Commonwealth Avenue, Boston, MA 02215, USA. (martinis@bu.edu)